

Detection of Tetraplex DNA and Detection by Tetraplex DNA

Shigeori TAKENAKA

Department of Applied Chemistry, Kyushu Institute of Technology, Kitakyushu 804-8550, Japan

G-quadruplex (G4) DNA forms through the gathering together of G-quartet planes formed with four guanine (G) bases. G4 DNA stabilizes with potassium ions (K^+) by coordination with the G-quartet center. Fluorometric G4 DNA carrying the fluorescence resonance energy transfer (FRET) chromophore pair at both termini has been applied for the fluorometric sensing or imaging of K^+ under a homogeneous aqueous medium. This system has realized non-conventional K^+ selectivity over the sodium ion (Na^+). The selectivity of the fluorescence G4 was converted to Na^+ from K^+ with a modification of its sequence. On the other hand, G4 DNA detection has been achieved in terms of cancer diagnosis because of a strong relationship of G4 DNA and cancer development. Ligands interacting with G4 are expected to have anti-cancer potential. In addition, fluorometric G4 ligands have been developed and tested as tools for the dynamic monitoring of G4 in living cells. Moreover, fluorometric G4 DNA has been utilized to evaluate the G4 ligand performance.

Keywords G-quadruplex (G4), potassium ion, sodium ion, fluorometric sensing, telomere DNA, telomerase, cancer diagnosis

(Received August 29, 2020; Accepted October 22, 2020; Advance Publication Released Online by J-STAGE October 30, 2020)

1 Introduction	9	4 Conclusions	14
2 Analysis Using G4 Structure	10	5 Acknowledgements	14
3 Analysis of G4 DNA	12	6 References	14

1 Introduction

Since the nineteenth century, it has been known that guanosine-rich nucleic acid residues turn into a gel under high millimolar concentrations.¹ In 1902, Bang proposed the structure of the tetraplex DNA (G4 DNA).¹ Later, the structure of the tetrameric unit containing four Gs (G-quartet) was analyzed and confirmed crystallographically by Gellert and co-workers in 1962.² Thereafter detailed G4 structures have been reported by many researchers.⁴ The G4 structure is formed by the folding of



Shigeori TAKENAKA is a Professor of Department of Applied Chemistry, Kyushu Institute of Technology. He received his PhD in 1988 at Kyushu University. He worked at Kyushu University as Research Associate (1987 - 1989) and as Associate Professor (1989 - 1991, 1996 - 2005). He also worked at Kyushu Institute of Technology as Associate Professor (1991 - 1996) and as Professor (2005 -). He was a visiting scientist for Prof. W. David Wilson, Georgia State University (1994 - 1995).

He was Director of Research Center for Bio-microsensing Technology (2006 - 2019). He has received 2019 Award for JSAC Award from the Japan Society for Analytical Chemistry, Japan. He is the author of 300 publications and 25 contribution books.

E-mail: shige@che.kyutech.ac.jp

single stranded DNA through stacking between the G-quartet planes and propeller (parallel), basket, chair, and hybrid type G4 structures, as shown in Fig. 1, which were known from the folding patterns. The center between two G-quartet planes fitted to the diameter of the K^+ and G4 structure was stabilized with K^+ . Despite this structural diversity, the selectivity for K^+ remains unaltered. Recently, the biological meaning of the G4 structure has been understood.⁵ There are 300000 potential G4 forming sequences with human genome sequencing. They contain telomere located at the end of the chromosome or regulation area of the cancer-related gene. Genes connected with nerves or the brain also contain a potential G4 structure. It is interesting that telomere DNA associated with cancer forms a G4 structure and telomerase interacting for telomere DNA is also contributing the G4 DNA structure in its gene expression. The G4 structure seems to be an important gene regulation function. A ligand which binds to the G4 DNA structure and stabilized its complex shows an anti-cancer activity, and is thus expected to be an anti-cancer drug with a low side effect.⁶ The G4 ligand having fluorescence change after being bound to G4 DNA is not only expected to be an anti-cancer drug, but also a fluorometric probe to analyze the rule of the G4 function under living cells. The analytical application of the G4 structure, cancer diagnosis or anti-cancer drug by analysis of the G4 structure, and fluorometric imaging reagents for G4 structure under living cell are reviewed in the paper.

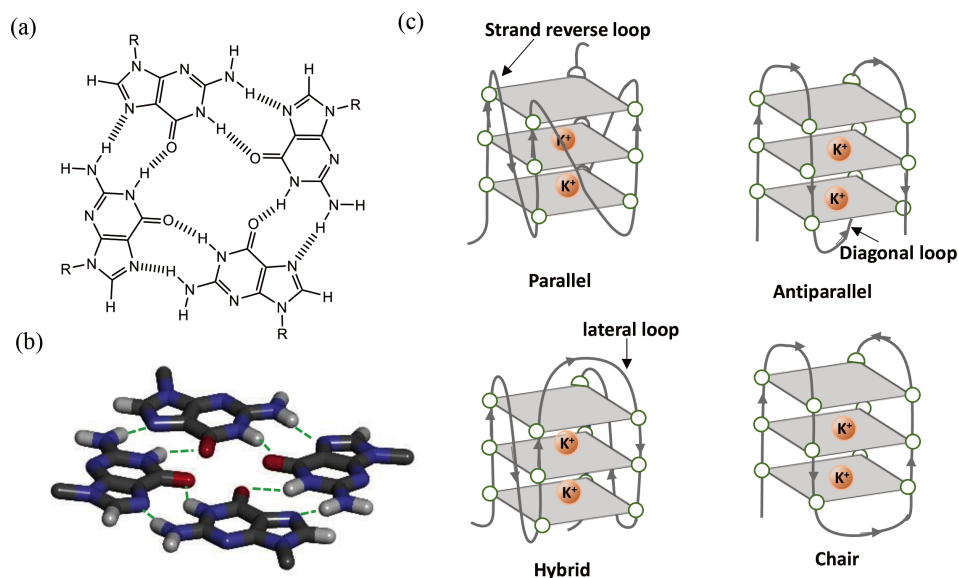


Fig. 1 (a) G-quartet where four guanine (G) residues act both as acceptors and donors of H-bonds in Hoogsteen geometry, (b) side view of G-quartet where Gs have a propeller twist angle, and (c) variety of detailed G-quadruplex (G4) structure.

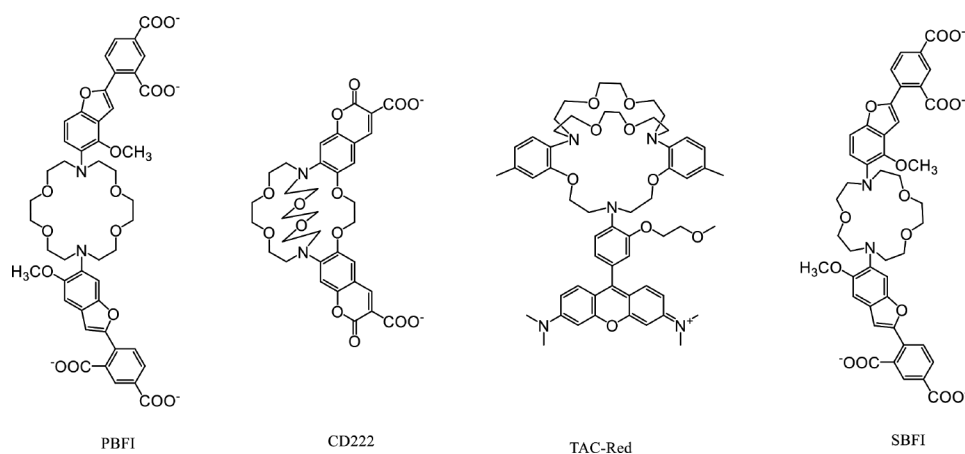


Fig. 2 Potassium ion indicators of PBF1, CD222, and TAC-Red and sodium ion indicator of SBF1.

2 Analysis Using G4 Structure

Potassium (K^+) and sodium (Na^+) ions exist under inter- and extra-cells and regulate the membrane potential. They have an integral role in nerve and brain action, and their aberrance encompasses severe disease, such as cardiac arrest.⁷ It is very important to analyze the K^+ and Na^+ concentrations in blood, and this analysis is among the health checking items. Until now, the K^+ and Na^+ concentrations were detected with an ion-selective electrode, and a high-performance ion-selective electrode has been developed. However, imaging reagents of K^+ and/or Na^+ under a homogenous aqueous medium have been delayed. The K^+ sensing reagent under an aqueous medium has been reported to be a basic skeleton of the crown ether coupled with a chromophore, and is not able to discriminate between K^+ and Na^+ because of their similar diameter, 266 and 190 pm, respectively. Figure 2 shows the typical K^+ sensing reagent, reported previously. Potassium-binding benzofuran isophthalate

(PBF1) and cryptant [2.2.2] have almost three-times preference of K^+/Na^+ .⁸ A fluorometric reagent carrying triazacryptand (TAC) skeleton realized approximately 30-times preference of K^+ over Na^+ coupled with the chromophore.⁹

On the other hand, the G4 DNA structure has stacked G-quartet planes and has a created space in the center between the G-quartet planes, incorporates K^+ with stabilization. The use of this characteristics leads to a K^+ sensing system. Takenaka and co-workers firstly reported the fluorometric K^+ sensing system.¹⁰ They synthesized oligonucleotide carrying a human telomere sequence and fluorescent resonance energy transfer (FRET) chromophore pairs of FAM and TAMRA (Fig. 3). This molecule folds to the G4 structure in the presence of K^+ , and the two chromophores come into proximity to generate an enhanced FRET signal. Since the amount of G4 formation is correlated with K^+ concentration, K^+ is a quantified FRET signal change under a homogeneous aqueous medium. A 43000-times selectivity of K^+ over Na^+ was realized in this system,¹⁰ whereas azacrown ether or troazacrown ether shows only a 30-times

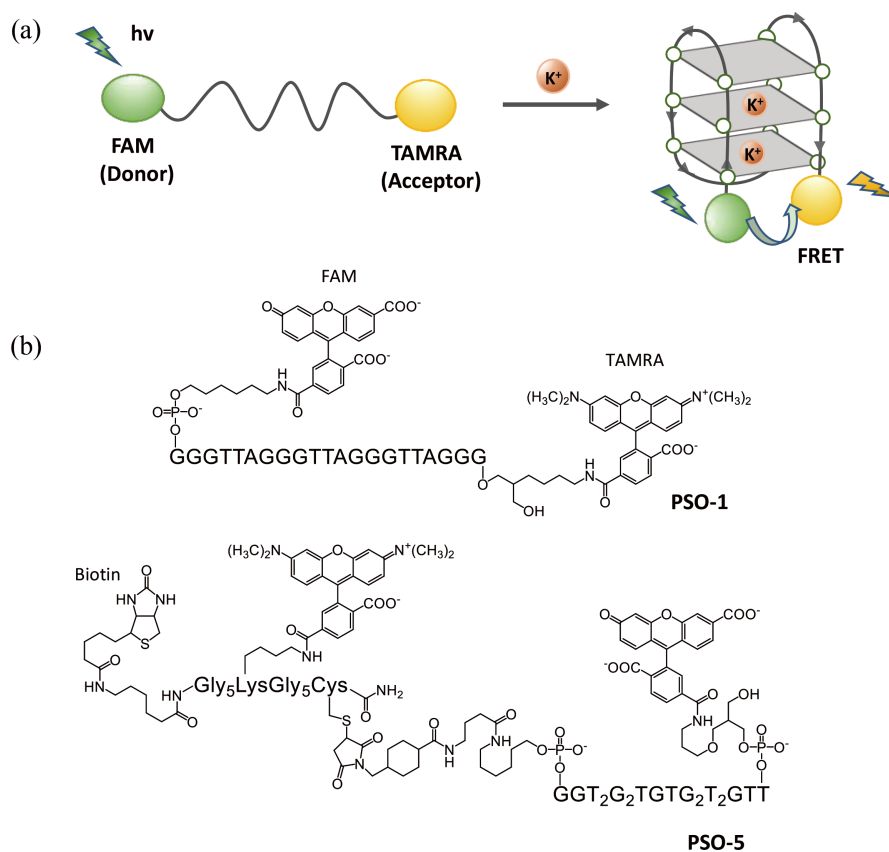


Fig. 3 (a) Principle of K^+ sensing based on G-quartet DNA and (b) chemical structures of PSO-1 and PSO-5.

preference of K^+/Na^+ as a binding constant ratio. This reagent was called a potassium sensing oligonucleotide (PSO-1). However, the FRET efficiency of the PSO-1 under Na^+ was higher than that under K^+ and thus PSO-1 was not suitable for detecting K^+ under an extracellular condition containing 140–150 mM Na^+ . Takenaka and co-workers tried to develop high-performance PSO derivatives, as reported previous review.¹¹ They chose a thrombin binding aptamer (TBA) sequence instead of a human telomere one in PSO derivatives. The dissociation constant of TBA was 0.29, or 158 mM for K^+ or Na^+ , respectively and the selectivity for K^+/Na^+ was 545-times.¹² PSO derivatives permitted the ratiometric fluorescence detection of K^+ in a buffered solution, and showed low photo-bleaching after undergoing laser irradiation, which is suitable for the real-time imaging of K^+ in a living cell. Takenaka and co-workers tried to carry out fluorescence K^+ imaging in a living cell by PSO. However, the PSO was concentrated into the nucleus and caused cell death. Since it is known that a G-rich DNA fragment binds to nucleolin, and leads to cell death, PSO should cause cell death in a similar way. Thus, a biotin unit was introduced in PSO, and the obtained PSO (PSO-5) was made into a 1:1 complex with avidin. Since avidin has four binding sites, this complex is remaining three sites and is filled with biotin-modified nuclear export signal peptide. Final complex was introduced into a cell by a bead loading method¹² and PSO-5 was succeeded the retaining in cytoplasm. Furthermore, the real-time monitoring of the K^+ efflux process was successfully achieved with PSO-5 after adding Amphotericin B and Ouabain as apoptosis inducer.¹² The dissociation constant of PSO-5 from K^+ was $K_d = 2.2$ mM.¹² Several types of K^+ sensing systems based on G4 formation have been reported after appearing in

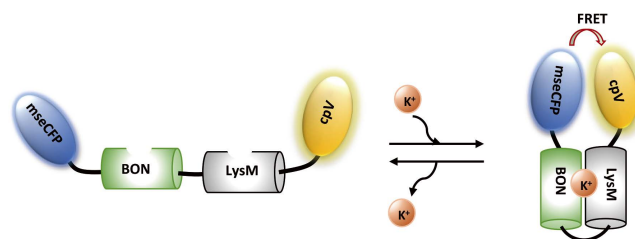


Fig. 4 Mechanism of K^+ sensing by FRET-based GEPIIs. GEPIIs undergoes folding in the presence of K^+ .

Takenakas' paper. They have been summarized in Juskowiak's review.¹³

Recently, selective fluorometric K^+ imaging was achieved with GEPIIs as a recombinant protein expressed in a cell.¹⁴ GEPIIs utilized a K^+ binding protein, Kbp, from bacteria recently detected (Fig. 4), where the BON domain and the Lysine motif (LysM) of Kbp were folded and surrounded around K^+ . GEPIIs linked between BON and LysM carrying fluorescent proteins (FPs) of the FRET pair and two domains were folded in the presence of K^+ , resulting in the approachable situation of two FPs, which enhanced the FRET signal. The fluorometric K^+ imaging of a living cell was realized by GEPIIs. The dissociation constant of GEPIIs for K^+ was reported to be $K_d = 0.16$ mM.¹⁴

On the other hand, fluorometric Na^+ imaging reported an azacrown-type chromophore, SBFI (short for sodium-binding benzofuran isophthalate) (Fig. 2).^{8,15} The selectivity of Na^+/K^+ as a binding constant ratio was 2.6-times in SBFI.

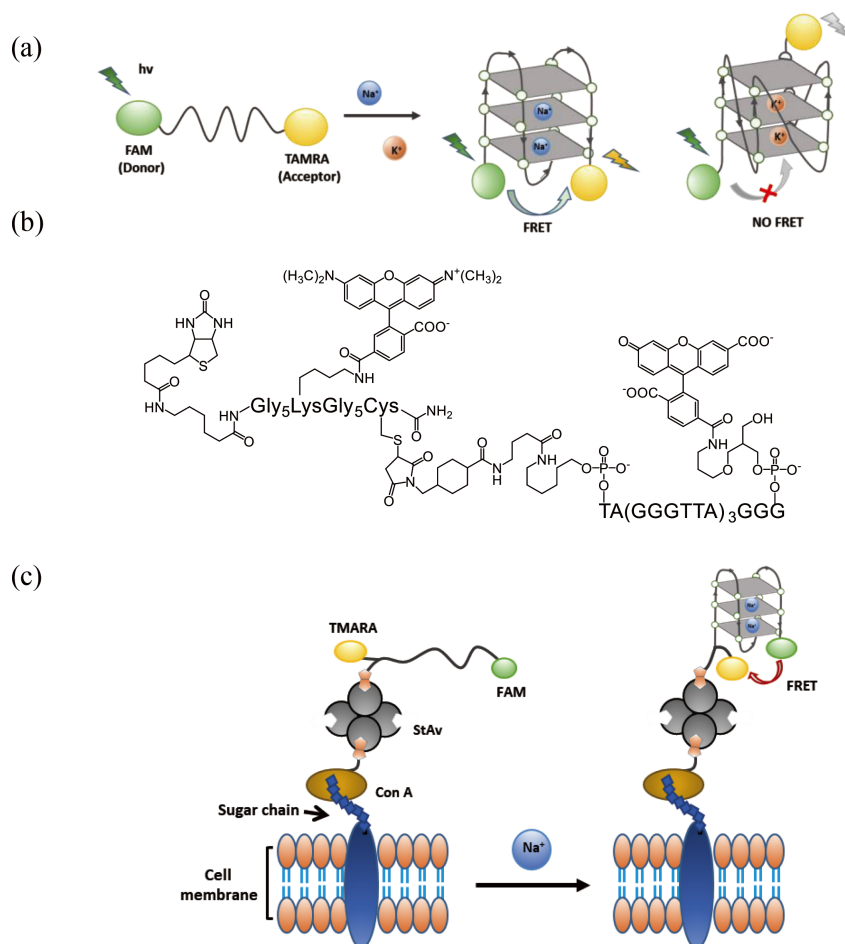


Fig. 5 (a) Principle of the fluorescence image of Na⁺ based on G-quartet formation of a human telomere DNA sequence, (b) designed peptide-oligonucleotide conjugate, and (c) the concept of immobilization of SSO on the cell surface.

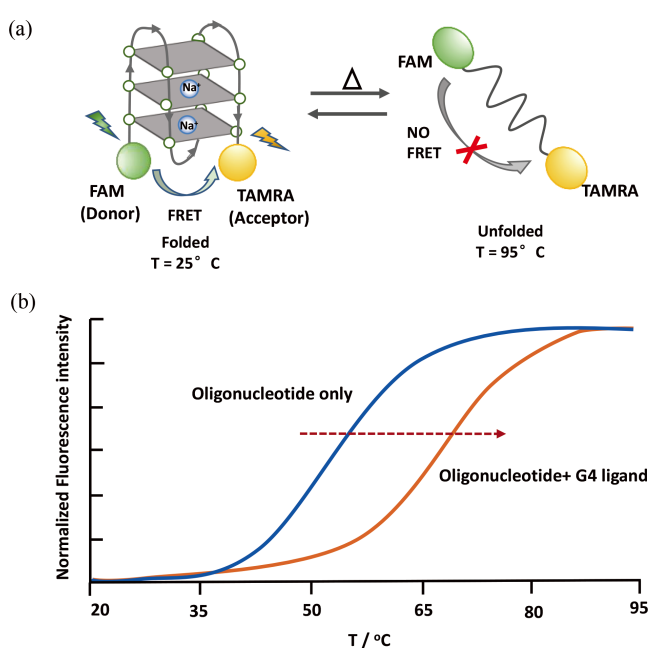


Fig. 6 (a) Conceptual diagram of FRET quenching under heating and (b) fluorescence change under heating in the absence and presence of G4 ligand.

Takenaka and co-workers developed an oligonucleotide carrying a FRET pair enhanced in the presence of Na⁺ by noticing the difference in the G4 structures in the presence of K⁺ or Na⁺: Basket and hybrid types were formed for Na⁺ and K⁺, respectively (Fig. 5). Using of a human telomere sequence, they constructed an oligonucleotide giving an enhanced FRET signal in the presence of Na⁺.¹⁶ They named this a sodium-sensing oligonucleotide, SSO.

PSO or SSO, developed by Takenaka's group, was stabilized in the presence of K⁺ or Na⁺, and this stabilization effect was monitored as the melting temperature, T_m , in a melting curve plotted FRET signal change against the temperature: the temperature in the presence of 1:1 of G4 and single stranded DNA is T_m . A comparative specification of G4 ligands was achieved by a difference of the T_m value in the absence and presence of the specific G4 ligand, as reported by Mergny's group (Fig. 6).¹⁷ Takenaka's group also reported a comparative specification of the G4 ligand with different type of G4 structure.¹⁸

3 Analysis of G4 DNA

A huge potential G4 forming site was known to exist on genome DNA as described before. The human telomere region at the termini of the chromosome has a repeating DNA sequence of

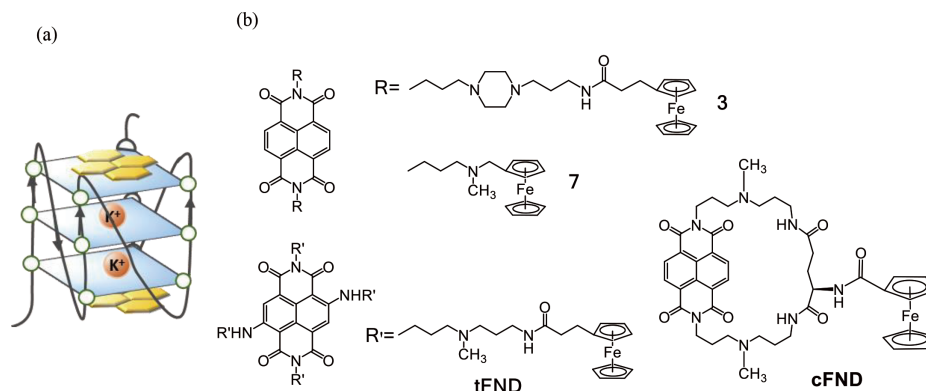


Fig. 7 (a) Complex model of naphthalene diimide with tetraplex DNA and (b) ferrocenylnaphthalene diimide (FND) derivatives as an electrochemical G4 binder.

TTAGGG, and this telomere DNA is constructed with a double-stranded structure from 4000 to 20000 base pairs (bp) and a single stranded structure of 200 bases (b) as G-tail.¹⁹ Generally, telomere DNA has 15000 bp in a fetus and 10000 bp from birth. It is said that a one-time cell division shortens the telomere by 20 - 170 bp, and because the telomere length reaches 5000 bp, the cell becomes senescent. Human tissue undergoes division 70-times, as an average value, whereas this limited number of division is in out of the rule in a germ or a stem cell. This indivisible cell is undergoing aging and subsequently the programmed cell death or apoptosis. When the cell becomes cancerous, this leads to the expression of telomerase as an elongation enzyme of telomere DNA, and moves to immortalization. Since the telomerase activity is known to show 80% of cancer, and this activity is observed at earlier stage of cancer, cancer diagnosis is achieved by telomerase detection. Although telomerase is an enzyme containing RNA fragments, and is weak for RNase existing in the ordinary environment, a simple and rapid detection system of telomerase activity has been required. The telomerase activity has been detected by a telomerase repeating amplification protocol (TRAP) assay: a sample solution is mixed with the telomerase substrate (TS)-primer and an elongated TS-primer with telomerase activity detected based on the number of the ladder in the gel electrophoresis after PCR amplification.²⁰ Since PCR is amplified, the area between the PCR primers and the elongated DNA has a repeating sequence of TTAGGG, one of the PCR primer was designed to hybridize a various position of TTAGGG, and therefore many ladders each 6 bp were observed under gel electrophoresis, and its activity was evaluated by how elongated ladder is observed. An improved TRAP assay has been reported as telomerase RCR ELISA, which is detected by the peroxidase enzymatic reaction after hybridization of a telomerase-specific probe with a PCR product in a TRAP assay.²¹ A method using Amplifluor RP primer was also reported.²² Amplifluor RP primer has a hairpin structure, with fluorophore and quencher dye. It shows no fluorescence, and the PCR product shows fluorescence with the PCR progress.

On the other hand, Takenaka and co-workers have been developing an electrochemical gene detection technique based on ferrocenylnaphthalene diimide (FND) coupled with a DNA probe-immobilized electrode.²³ FND is a threading intercalator, where two substituents of FND are located in major and minor grooves after being bound to double-stranded DNA, and the complex was stabilized by the anchoring of both substituents. Since this stabilization is observed only for double-stranded

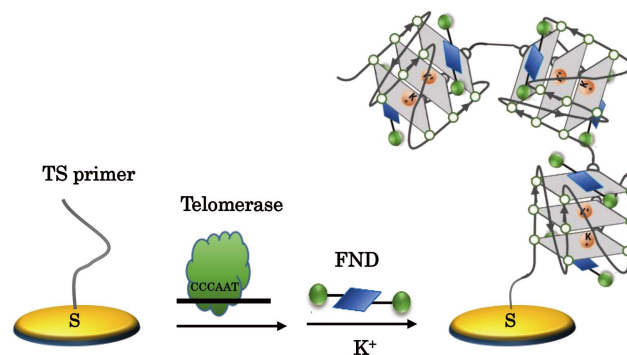


Fig. 8 Principle of electrochemical telomerase assay (ECTA) using FND.

DNA, not a single-stranded one, FND discriminates the double-stranded DNA from the single-stranded one. A hybrid of target DNA with a DNA probe on the electrode was electrochemically detected by FND. Recently, naphthalene diimide has been known to bind to G4 DNA.²⁴ This was derived from effective stacking between electron-deficient naphthalene diimide and an electron-rich G-quartet plane. Takenaka's group found that FND3 and FND7 (Fig. 7) as suitable FNDs for tetraplex DNA binding is possible and established an electrochemical telomerase assay coupled with a TS-primer-immobilized electrode (Fig. 8).²⁵ In this assay, the elongated DNA on the electrode-formed G4 structures to be detected by FND electrochemically, which obtained an indirect detection of the telomerase activity. This system was applied to oral cancer diagnosis by corroborating research with a surgeon dentist of Kyushu Dental University. A high sensitivity diagnosis of oral cancer was achieved with a non-invasive treatment of only brushing within the oral cavity, and the diagnosis was realized under the precancerous state of oral cancer.^{26,27} Takenaka's group prepared TS-primer-immobilized electrode and electrochemically detected the amount of FND concentrated on the electrode, which bound to G4 DNA elongated with telomerase. Takenaka's group developed naphthalene diimide carrying four ferrocenyl substituents²⁸ and cyclic ferrocenylnaphthalene diimide²⁹ as a further high-performance electrochemical G4 ligand.

The DNA amount of the elongated TS-primer immobilized on the substrate with telomerase detected by SPR³⁰ or a field-effect

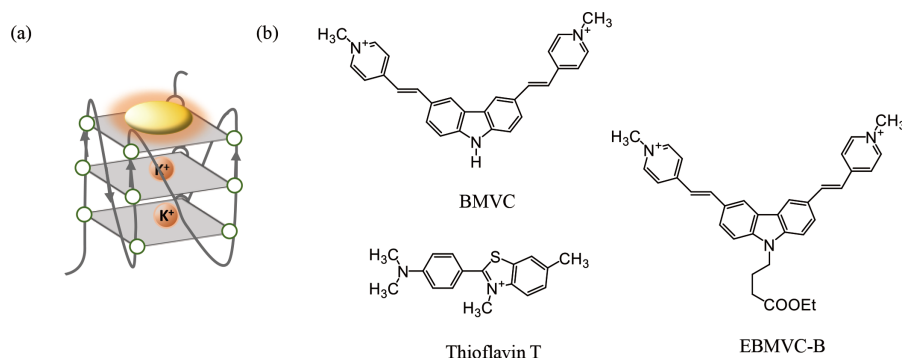


Fig. 9 (a) Enhanced fluorescence of G4 ligand after bound to G-quartet DNA and (b) G4 ligands which enhanced their fluorescence after bound to tetraplex DNA.

transistor (FET)³¹ was reported as different assay technique. Since the elongated DNA with telomerase is containing many G, the telomerase activity was detected by the oxidation current of G indirectly.³²

The ligand that enhances its fluoresce after being bound to G4 DNA has a potential for fluorometric G4 imaging in a living cell. Chang and co-workers³³ firstly synthesized 3,6-bis(1-methyl-4-vinylpyridium)carbazole diiodide (BMVC) as such G4 ligand (Fig. 9). This molecules has aromatic residues connected through a carbon-carbon single bond and accommodated to G-quartet having a propeller twist angle to give the best stacking. Free rotation of the single bond was repressed by this stacking, and also suppressed the thermal deactivation, resulting in enhanced fluorescence. Cheng and co-workers successfully achieved the fluorometric imaging of G4 in mitochondria in a living cell using BMVC.³⁴ Furthermore, Chang developed an evaluation technique of the G4 ligand by the competition of BMVC in a cell.³⁵ Other G4 ligands based on the concept of BMVC have been reported, as summarized review.³⁶ Thioflavin T has two aromatic residues connected through a carbon-carbon single bond, like a BMVC and formed association complex in an aqueous medium resulting in its fluorescence quenching. Since single Thioflavin T binds to G4 DNA, the quenching was resolved and give a fluorescence. A near-infrared G4 ligand is of particular interest in terms of reducing cell damage by laser irradiation.³⁸

It is expected that the G4 ligand, which shows fluorescence after being bound to G4, was utilized K⁺ sensing because of G4 formation with K⁺. Yang *et al.*³⁹ realized by EBMVC-B (Fig. 9) also known as two-photon excitation chromophore. This system shows a linear change of the K⁺ concentration from 0.5 to 10 mM, and no effect of other ions, such as Na⁺, Ca²⁺, Mg²⁺, and Zn²⁺, which are often observed in blood. They successfully detected K⁺ as a physiologically relevant concentration.

4 Conclusions

This review summarizes an analytical application connected with G4, known as a non-canonical DNA structure: detection by G4 and the detection of G4. Although recent progress concerning of G4 research was accelerated, it is still not clear about the fine G4 structure in a cell; however, such a fine G4 structure becomes important with understanding of the detailed gene action. It is important for developing anti-cancer drug without side effects and G4 ligands might provide such drug. It will also become important to develop a new technique to

analyze the function of the G4 DNA structure in living cells, depending on a subtle difference of the G4 structure.

5 Acknowledgements

I appreciate the significant contribution made by researchers who appear in the reference papers of Takenaka's group. I thank Dr. Zou Tingting for preparing a conceptual diagram of figures according to my idea and thank Dr. Shinobu Sato for her engaging discussions and support.

6 References

1. W. Guschlbauer, J. F. Chantot, and D. Thiele, *J. Biomol. Struct. Dyn.*, **1990**, 8, 491.
2. M. Gellert, M. N. Lipsett, and D. R. Davies, *Proc. Natl. Acad. Sci. U. S. A.*, **1962**, 48, 2013.
3. I. Bang, *Biochem. Z.*, **1910**, 26, 293.
4. S. Burge, G. N. Parkinson, P. Hazel, A. K. Todd, and S. Neidle, *Nucl. Acids Res.*, **2006**, 34, 195402.
5. V. S. Chambers, G. Marsico, J. M. Boutell, M. D. Antonio, G. P. Smith, and S. Balasubramanian, *Nat. Biotechnol.*, **2015**, 33, 877.
6. A. P. Saraswati, N. Relitti, M. Brindisi, S. Gemma, D. Zisterer, S. Butini, and G. Campiani, *Drug Discovery Today*, **2019**, 24, 1370.
7. P. J. S. Smith and J. Trimarchi, *Am. J. Physiol. Cell Physiol.*, **2001**, 280, C1.
8. H. Szmecinski and J. R. Lakowicz, *Sens. Actuators, B*, **1999**, 60, 8.
9. P. Padmawar, X. Yao, O. Bloch, G. T. Manley, and A. S. Verkman, *Nat. Methods*, **2005**, 2, 825.
10. H. Ueyama, M. Takagi, and S. Takenaka, *J. Am. Chem. Soc.*, **2002**, 124, 14286.
11. S. Takenaka and B. Juskowiak, *Anal. Sci.*, **2011**, 27, 1167.
12. K. Ohtsuka, S. Sato, Y. Sato, K. Sota, S. Ohzawa, T. Matsuda, K. Takemoto, N. Takamune, B. Juskowiak, T. Nagai, and S. Takenaka, *Chem. Commun.*, **2012**, 48, 4740.
13. B. Juskowiak, *Anal. Chim. Acta*, **2006**, 568, 171.
14. H. Bischof, M. Rehberg, S. Stryeck, K. Artinger, E. Eroglu, M. Waldeck-Weiermair, B. Gottschalk, R. Rost, A. T. Deak, T. Niedrist, N. Vujic, H. Lindermuth, R. Prassl, B. Pelzmann, K. Groschner, D. Kratky, K. Eller, A. R. Rosenkranz, T. Madl, N. Plesnila, W. F. Graier, and R. Malli, *Nat. Commun.*, **2017**, 18, 1422.

15. A. Minta and R. Y. Tsien, *J. Biol. Chem.*, **1989**, *264*, 19449.
 16. S. Sato, Y. Imaichi, Y. Yoshimura, K. Nakazawa, and S. Takenaka, *Anal. Sci.*, **2019**, *35*, 85.
 17. J.-L. Mergny and J.-C. Maurizot, *ChemBioChem*, **2001**, *2*, 124.
 18. Md. M. Islam, S. Fujii, S. Sato, T. Okauchi, and S. Takenaka, *Molecules*, **2015**, *20*, 10963.
 19. D. T. A. Eisenberg, *Am. J. Hum. Biol.*, **2011**, *23*, 149.
 20. N. W. Kim, M. A. Piatyszek, K. R. Prowse, C. B. Harley, M. D. West, P. L. C. Ho, G. M. Coviello, W. E. Wright, S. L. Weinrich, and J. W. Shay, *Science*, **1994**, *266*, 2011.
 21. A. Hooks, H. H. Hepp, S. Kaul, T. Ahlert, G. Bastert, and D. Wallwiener, *Int. J. Cancer*, **1998**, *79*, 8.
 22. H. Uehara, G. Nardone, I. Nazarenko, and R. J. Hohman, *BioTechniques*, **1999**, *26*, 552.
 23. S. Takenaka, *Bull. Chem. Soc. Jpn.*, **2001**, *74*, 217.
 24. V. Pirota, M. Nadai, F. Doria, and S. N. Richter, *Molecules*, **2019**, *24*, 426.
 25. S. Sato, H. Kondo, T. Nojima, and S. Takenaka, *Anal. Chem.*, **2005**, *77*, 7304.
 26. K. Mori, S. Sato, M. Kodama, M. Habu, O. Takahashi, T. Nishihara, K. Tominaga, and S. Takenaka, *Clin. Chem.*, **2013**, *59*, 289.
 27. M. Hayakawa, S. Sato, I. Diala, M. Kodama, K. Tomoeda-Mori, K. Haraguchi, K. Tominaga, and S. Takenaka, *Electroanalysis*, **2016**, *28*, 503.
 28. S. Sato, A. Kajima, H. Hamanaka, and S. Takenaka, *J. Organomet. Chem.*, **2019**, *897*, 107.
 29. S. Kaneyoshi, T. Zou, S. Ozaki, R. Takeuchi, A. Udou, T. Nakahara, F. Fujimoto, S. Fujii, S. Sato, and S. Takenaka, *Chem.—Eur. J.*, **2020**, *26*, 139.
 30. C. Maesawa, T. Inaba, H. Sato, S. Iijima, K. Ishida, M. Terashima, R. Sato, M. Suzuki, A. Yashima, S. Ogasawara, H. Oikawa, N. Sato, K. Saito, and T. Masuda, *Nucl. Acids Res.*, **2003**, *31*, e4.
 31. E. Sharon, R. Freeman, M. Riskin, N. Gil, Y. Tzfati, and I. Willner, *Anal. Chem.*, **2010**, *82*, 8390.
 32. U. Eskiocak, D. Ozkan-Ariksoysal, M. Ozsoz, and H. A. Oktem, *Anal. Chem.*, **2007**, *79*, 8807.
 33. C.-C. Chang, J.-Y. Wu, C.-W. Chien, W.-S. Wu, H. Liu, C.-C. Kang, L.-J. Yu, and T.-C. Chang, *Anal. Chem.*, **2005**, *75*, 6177.
 34. W.-C. Huang, T.-Y. Tseng, Y.-T. Chen, C.-C. Chang, Z.-F. Wang, C.-L. Wang, T.-N. Hsu, P.-T. Li, C.-T. Chen, J.-J. Lin, P.-J. Lou, and T.-C. Chang, *Nucl. Acids Res.*, **2015**, *43*, 10102.
 35. T.-Y. Tseng, I.-T. Chu, S.-J. Lin, J. Li, and T.-C. Chang, *Molecules*, **2019**, *24*, 35.
 36. P. Chilka, N. Desai, and B. Datta, *Molecules*, **2019**, *24*, 752.
 37. J. Mohanty, N. Barooah, V. Dhamodharan, S. Harikrishna, P. I. Pradeepkumar, and A. C. Bhasikuttan, *J. Am. Chem. Soc.*, **2013**, *135*, 367.
 38. Y. V. Suseela, N. Narayanaswamy, S. Pratihari, and T. Govindaraju, *Chem. Soc. Rev.*, **2018**, *47*, 1098.
 39. L. Yang, Z. Qing, C. Liu, Q. Tang, J. Li, S. Yang, J. Zheng, R. Yang, and W. Tan, *Anal. Chem.*, **2016**, *88*, 9285.
-